

How Single-Walled Carbon Nanotubes are Transformed into Multiwalled Carbon Nanotubes during Heat Treatment

Byungcheon Yoo, Ziwei Xu, and Feng Ding*



Cite This: *ACS Omega* 2021, 6, 4074–4079



Read Online

ACCESS |



Metrics & More

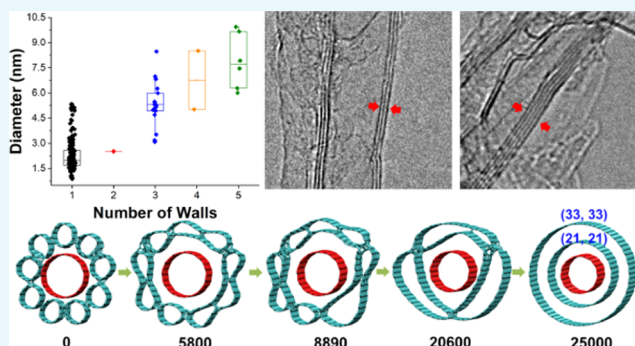


Article Recommendations



Supporting Information

ABSTRACT: High-pressure carbon monoxide (HiPCO) single-walled carbon nanotubes (SWCNTs) were heat treated at high temperatures from 1700 to 3000 °C. During the heating below 2500 °C, the diameters of the SWCNTs gradually increase from ~1.0 to >1.5 nm, and at the temperatures higher than 2500 °C, double-, triple-, multiwalled carbon nanotubes (MWCNTs) appear as a consequence of the coalescence of SWCNT bundles. It is surprising that most MWCNTs have odd number of walls, such as 3 or 5. The even–odd number effect agrees well with the mechanism of SWCNT bundle coalescence proposed by López, M. J. et al. [*Phys. Rev. Lett.* **2002**, 89, 255501], in which an SWCNT that templated the layer by layer coalescence of surrounding SWCNTs is responsible for the enrichment of MWCNTs with odd number of walls. This study confirms the mechanism of SWCNT bundle coalescence, discovers an interesting odd–even number of walls effect in the consequent MWCNTs, and suggests that it is possible to obtain structure-controllable MWCNTs via SWCNT bundle coalescence.



INTRODUCTION

Carbon nanotubes (CNTs) have been considered as novel materials for many important applications due to their outstanding properties, such as high electric and thermal conductivities, very high thermal stability, and outstanding mechanical strength since their discovery in 1991.¹ A great deal of effort has been dedicated to controlling the structure of CNTs as well as their properties^{2–4} either during synthesis or by post-synthesis treatment^{5–8} for various applications.

Particularly, Bronikowski et al. introduced a high-pressure carbon monoxide (HiPCO) method to synthesize single-walled carbon nanotubes (SWCNTs), in which Fe(CO)₅ and high-pressure CO were introduced into a tube furnace as catalysts to continuously produce SWCNTs with narrow diameters of ~0.7 to 1.2 nm.⁸

Heat treatment of SWCNTs has been considered an important post-growth technique to tailor the structure and properties of the CNTs. In 1997, Nikolaev et al. reported the SWCNT diameter doubling as a consequence of SWCNT coalescence by the heat treatment at a temperature of 1400 °C.⁹ The driving force of the SWCNT coalescence is known as the reduced strain energy and the SWCNTs with exactly the same chiral angle can coalesce seamlessly in a bundle. In 2001, Yudasaka et al. heat treated the HiPCO SWCNTs from 1000 to 2000 °C for 5 h in vacuum and the Raman spectra showed that the diameters of SWCNTs became larger and larger gradually.¹⁰ They proposed another mechanism of the SWCNT structure change during heat treatment: the diameter

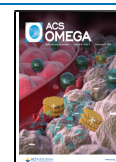
of an SWCNT can gradually change by self-reconstruction. In 2002, Méténier et al. observed the formation of multiwalled CNTs (MWCNTs) after the heat treatment of SWCNT bundles at a temperature higher than 2200 °C.¹¹ Later, a mechanism of SWCNT bundle coalescence, many SWCNTs coalesce around the central SWCNT, was proposed to understand the experimental observation.¹²

Here, we report an experimental study of the heat treatment of HiPCO SWNTs in a broader temperature range of 1700–3000 °C with a rapid joule heating system, which allows the SWCNT samples to be heated to the targeted temperature within 10 s. Our study reveals that the diameter of SWCNTs keeps on increasing with the increase of the temperature until 2500 °C and then MWCNTs start to form at higher temperatures. A careful measurement of the MWCNTs showed that most MWCNTs have odd number of walls, such as 3 or 5, and only few of them have even number of walls. Based on the previously proposed mechanism of the central SWCNT that templated the coalescence of surrounding SWCNTs, we successfully explained the odd–even effect and

Received: December 16, 2020

Accepted: January 15, 2021

Published: January 26, 2021



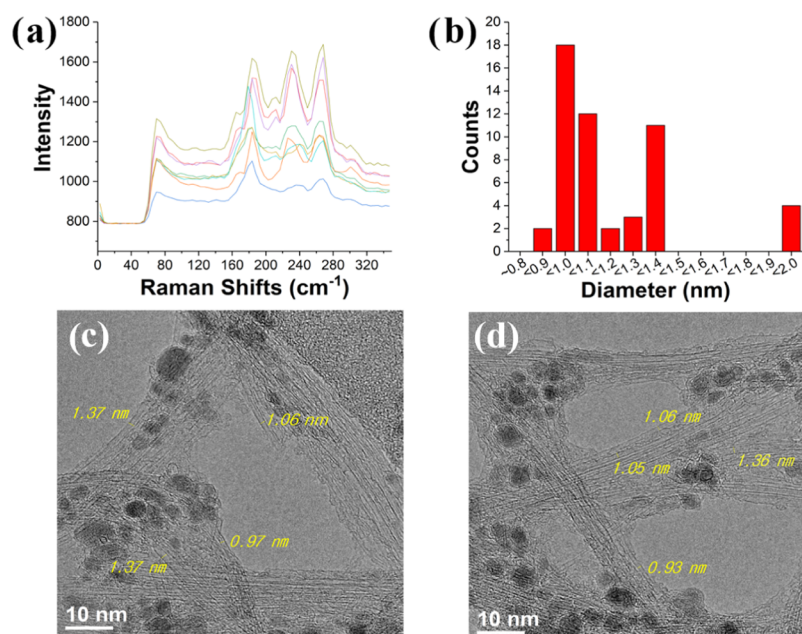


Figure 1. Characterization of pristine HiPCO SWCNTs. (a) RBM peaks; (b) diameter distribution; and (c, d) TEM images.

further confirmed the previously proposed mechanism of SWCNT bundle coalescence.

RESULTS AND DISCUSSION

The diameters of pristine HiPCO SWCNTs can be determined by the radial breathing mode (RBM) of the Raman spectra and transmission electron microscopy (TEM) images, as shown in Figure 1. The dominant Raman RBM peaks of the pristine sample are 183, 231, and 267 cm^{-1} . Using the equation $d = 248/\omega_{\text{RBM}}$,¹⁷ these peaks correspond to diameters of 1.35, 1.07, and 0.93 nm, respectively, as shown in Figure 1b. From the TEM images (Figure 1c,d), we can see that most pristine SWCNTs have diameters in the range of 0.9–1.3 nm and are bundled together. The number of SWCNTs in a bundle ranges from a few to many tens.

In Figure 2a, the dominating RBM peaks of the pristine SWCNT sample and those heated to different temperatures

are marked by arrows. Below a temperature of 2000 $^{\circ}\text{C}$, the positions of the three dominating RBM peaks, 183, 231, and 267 cm^{-1} , remain the same but the high-frequency peaks (231 and 267 cm^{-1}) keep on decreasing with the increase of the temperature, implying that smaller SWCNTs gradually become larger and larger but the largest ones remain unchanged. It is important to note that there are no RBM peaks of SWCNTs with diameters of ~ 2 nm, which means that the gradual disappearance of the small-diameter SWCNTs is not a consequence of SWCNT doubling or coalescence. So, we believe that the disappearance of the small SWCNTs at temperatures lower than 2000 $^{\circ}\text{C}$ is mainly caused by the reconstruction of the SWCNTs. At a temperature of 2300 $^{\circ}\text{C}$, new RBM peaks (144 and 169 cm^{-1}) emerge and the corresponding diameters of the new SWCNTs (1.46 and 1.72 nm) are very close to the double of the diameters of the smallest HiPCO SWCNTs, 0.7–0.8 nm, which implies that the smallest SWCNTs in the HiPCO sample start to coalesce at 2300 $^{\circ}\text{C}$. On further increasing the temperature to 2700 $^{\circ}\text{C}$, an RBM peak, 115 cm^{-1} , which corresponds to the SWCNT with a diameter of 2.15 nm appears. So, we believe that the doubling of large SWCNTs requires a high temperature.

In summary, we have observed two mechanisms of the HiPCO SWCNT structure transformation during heat treatment: the diameter of small SWCNTs can be gradually enlarged by the structural transformation and the coalescence of the SWCNTs occurs at higher temperatures. Besides, our study also confirms that both the structural transformation and the coalescence of larger SWCNTs require a higher temperature than those for smaller ones.

The G peaks (1580 cm^{-1}) of the pristine and heat-treated SWCNTs are shown in Figure 2b. We can clearly see that the left shoulder of the G peak (~ 1500 cm^{-1}) gradually decreases with the increase of the heat treatment temperature and eventually disappears at 3000 $^{\circ}\text{C}$. This agrees with the disappearance of the small-diameter SWCNTs and the metallic SWCNTs, which are known less stable than the semi-conducting ones.¹⁸

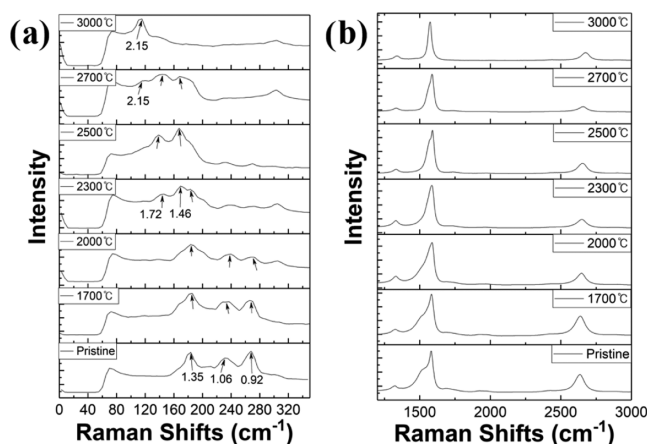


Figure 2. Raman spectra of the HiPCO pristine sample heat treated at different temperatures (estimated diameters (nm) from radial breathing mode are indicated). (a) Radial breathing mode and (b) G and D peaks.

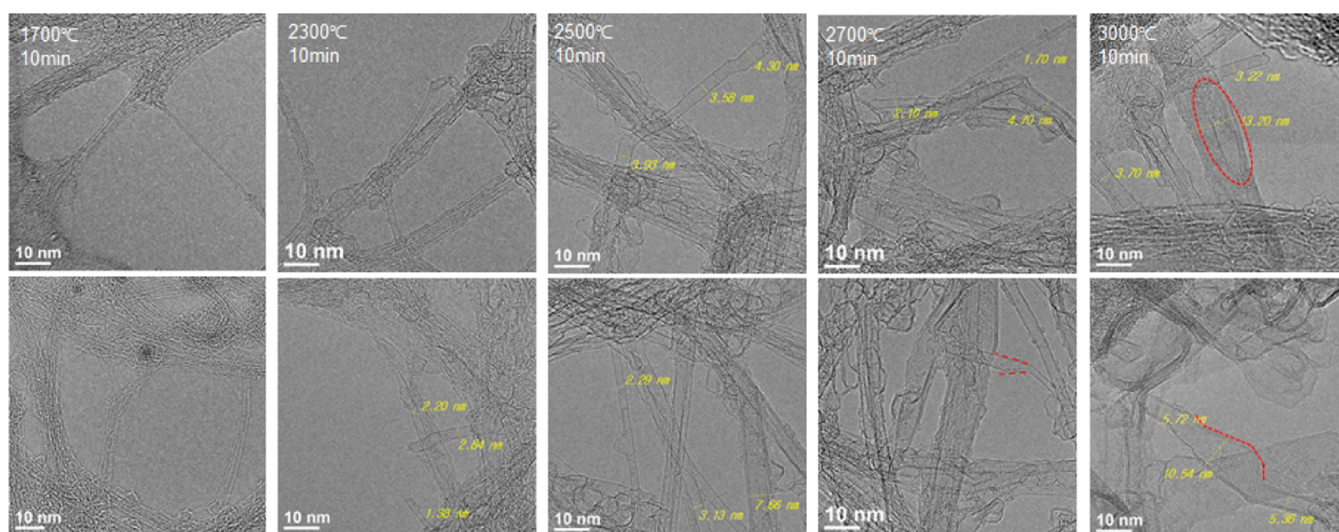


Figure 3. TEM images of HiPCO SWCNTs after heat treatment at various temperatures (red dotted marks show unique features caused by heat treatment).

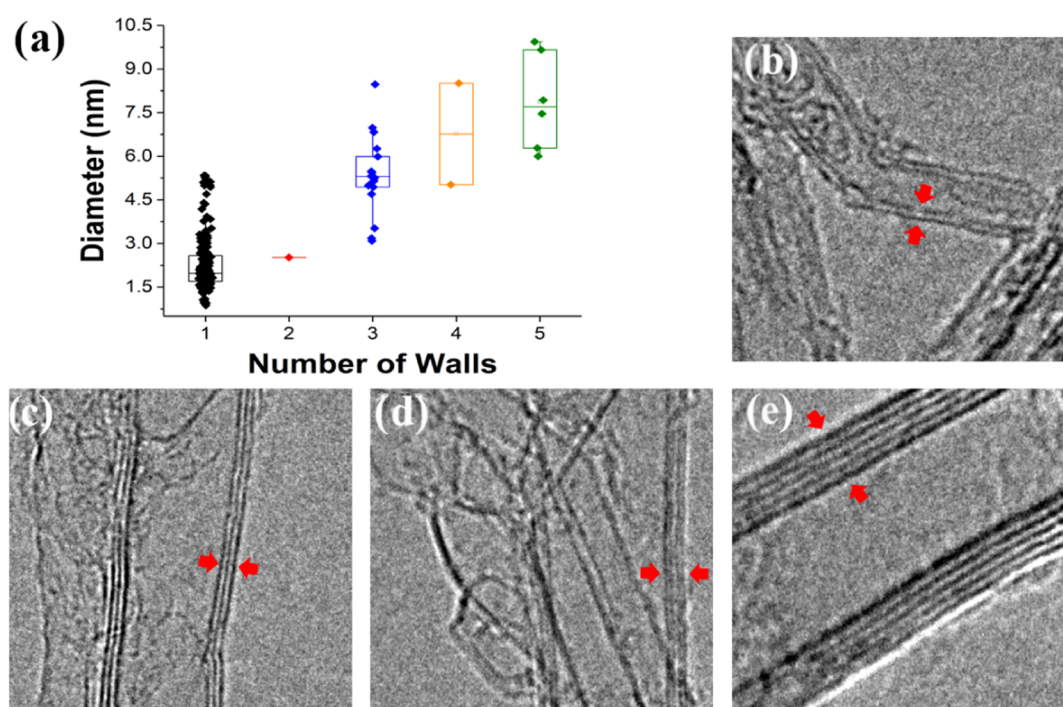


Figure 4. (a) Statistics about the diameter and number of nanotube walls after heat treatment at 2700 °C. TEM images with (b) double-walled, (c) triple-walled, (d) 4-walled, and (e) 5-walled carbon nanotubes.

The heated CNT samples were further characterized by transmission electron microscopy (TEM) (Figure 3). Compared to the pristine sample (Figure 1c,d), Figure 3 clearly shows that metal particles disappear quickly during heat treatment. Although the metal clusters disappear at 1700 °C, the diameter and quality of original SWCNTs are not changed as shown by the Raman RBM peaks and the G/D ratio (Figure 2a,b). This agrees well with the previous report that Fe particles cannot affect the structural changes of the SWCNTs at higher temperatures.¹⁹ Consistent with the results shown in the Raman spectra (Figure 2a), the diameters of the SWCNTs remain the same at 1700 °C or lower temperatures. At 2300 °C, all CNTs are SWCNTs, although their diameters are significantly larger than those of the pristine ones. From 2500

°C, more and more MWCNTs start to appear and the number of walls becomes larger and larger. Besides the straight CNTs, structures like the bending CNT junctions and CNTs with irregular diameters and varying number of walls are frequently seen (the red dotted line in Figure 3).

Figure 4a shows the correlation between diameters and the number of walls of some typical CNTs after heat treatment at 2700 °C, and Figure 4b–e shows some typical MWCNTs with different number of walls. First, we can see that there is no CNT with a diameter smaller than 1 nm and the diameters of the new CNTs are distributed in a much broader range, from 1 to 10 nm. The diameters of SWCNTs range from 1 to 5 nm and those of triple- and 5-walled CNTs range from 3 to 8 and 6 to 10 nm, respectively. From the TEM images (Figure 3), we

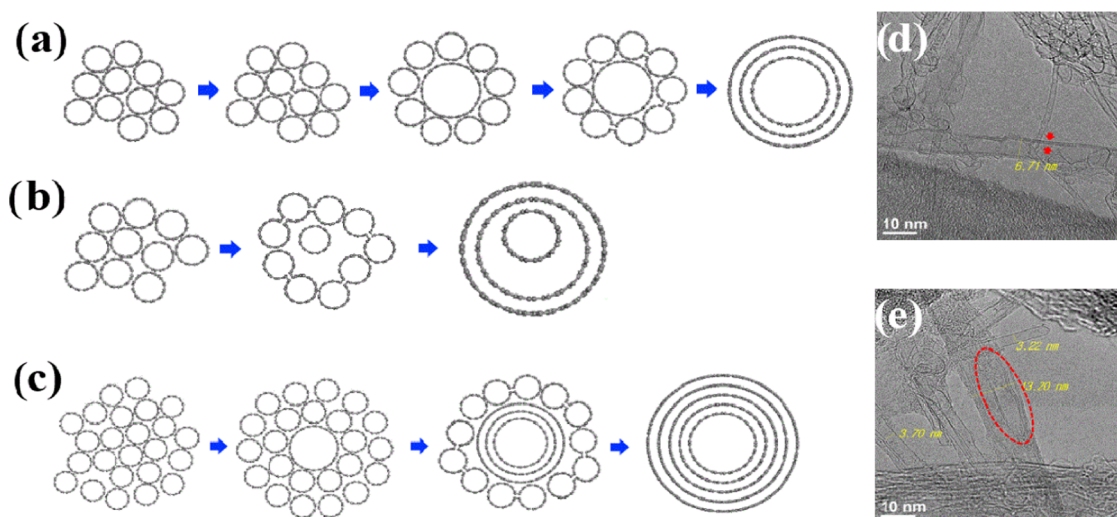


Figure 5. (a, d) Mechanism of transformation into a triple-walled tube and the TEM image; (b, e) mechanism of CNT coalescence that has different diameters in the same tube and the TEM image; and (c) mechanism to transform into a 5-walled tube in more bundles.

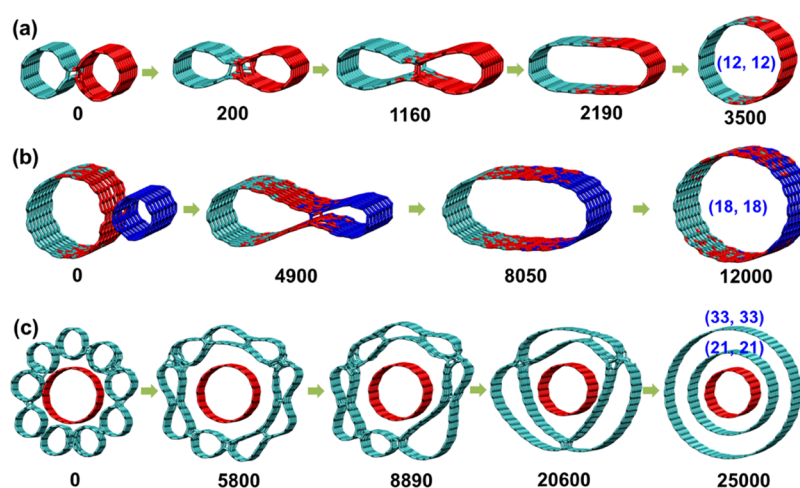


Figure 6. Coalescence of (6,6) SWCNTs: (a) (6,6) + (6,6) SWCNTs, (b) (6,6) + (12,12) SWCNTs, and (c) spontaneous coalescence of nine (6,6) SWCNTs around a dummy (12,12) SWCNT. The GSW step is given below each snapshot.

can see that the average number of tubes in each bundle is around 2–5, which is significantly smaller than that of the pristine bundles. This is clear evidence that the SWCNT coalescence in a bundle occurred during heat treatment. To form a triple-walled CNT of ~ 5 nm, the coalescence of 15 SWCNTs of ~ 1 nm is required. So, we believe that the existence of large SWCNT bundles in the pristine HiPCO sample is responsible for the formation of large diameter MWCNTs.

It is surprising that the number of double-walled and 4-walled CNTs are very few. Among the observed 180 CNTs, we have observed only one DWCNT and two 4-walled CNTs, but 17 triple-walled CNTs and six 5-walled CNTs are clearly identified (Figure 4a). This observation implies that the formation of CNTs with even number of walls is forbidden during the coalescence of SWCNT bundles. So, why is this the case?

It is important to note that the coalescence of two SWCNTs and sequential coalescence of many SWCNTs always lead to a large SWCNT. So, the formation of an MWCNT must be different from SWCNT doubling observed by Nikolaev et al.⁹ In 2002, López et al. proposed a mechanism of the MWCNT

growth, in which the coalescence of a 7-SWCNT bundle was explored by molecular dynamic simulation.¹² During the molecular dynamic simulation, the spontaneous coalescence of the six surrounding SWCNTs around the central one finally leads to a triple-walled CNT. Following such a mechanism, we plot two coalescence processes of SWCNT bundles shown in Figure 5a,b, one of which results in a triple-walled CNT with a short wall–wall distance and another one leads to a triple-walled CNT with a large wall–wall distance. It is interesting to note that both types of MWCNTs have been observed in our TEM images (Figure 5d,e). Such a mechanism can be extended to explain the formation of 5-walled CNTs as well, where the further coalescence of the surrounding SWCNTs around a triple-walled CNT finally leads to a 5-walled MWCNT. The key part of the mechanism is that the sequential coalescence of a few SWCNTs always leads to an enlarged SWCNT and the spontaneous coalescence of the surrounding SWCNTs will add two layers to the SWCNT every time. So, MWCNTs with even number of walls are forbidden in such a coalescence process. Besides the formation of MWCNTs, the formation of various CNT junctions can also be easily explained.

To confirm our proposed mechanism above, we performed energy-driven Monte Carlo (EDKMC) simulations on three typical scenarios of the SWNT coalescence, as shown in Figure 6. Figure 6a,b shows the sequential coalescence of three SWNTs of (6,6) chirality. As shown in Figure 6a, at first, two (6,6) SWCNTs connect to each other with a neck formed initially. Similar to the previous studies,^{13–15} the whole structure transformation is driven by the fast decrease of the high curvature energy of the system. For this reason, the neck section with ultrahigh curvature energy becomes fatter and fatter and the C–C bonds connecting the up and bottom carbon layers break gradually. Finally, a perfect single-walled carbon nanotube of (12,12) is formed at the 3500 GSW step. Figure 6b shows the coalescence of the third (6,6) SWCNT with the (12,12) SWCNT just formed at the 12 000 GSW step. Obviously, the ultimate structure is still a single-walled carbon nanotube with a larger size, which agrees well with our proposed result on the sequential coalescence. The spontaneous coalescence of an SWCNT loop around the central SWCNT, however, will lead to an MWCNT with odd carbon walls. As shown in Figure 6c, the nine (6,6) SWCNTs around the (12,12) SWCNT can merge together with the nine necks and disappear gradually. At the 20 600 GSW step, the outer and inner walls start to separate with only few bonds connected. Finally, at the 25 000 GSW step, a triple-walled carbon nanotube is formed. Of course, the wall–wall distance depends on the size of the central SWCNT. If the size of the central SWCNT is too small, the uneven wall–wall distance appears.

CONCLUSIONS

We studied the structure and diameter changes in HiPCO SWCNTs during heat treatment. The diameters of the tubes first gradually enlarged at 2000 °C and then the coalescence of small SWCNT bundles led to large SWCNTs but the coalescence of large SWCNT bundles (with number of SWCNTs >10) led to MWCNTs with odd number of walls at temperatures higher than 2500 °C. With this experimental result, we further demonstrated the previously discussed mechanism to clear through the EDKMC simulation works. Also, we observed that some SWCNTs transformed into various nanostructures. It is clear that SWCNTs are not very stable at a high temperature and the structure transformed from the SWCNTs highly depends on the environment and conditions of annealing. Based on these observations, we suggested a novel mechanism of SWCNT bundle coalescence, which led to MWCNTs with odd number of walls during heat treatment. It is worth studying further because it can be a novel method to control the diameter and number of walls for various applications, such as in energy storage, nano-composites, etc.

EXPERIMENTAL AND SIMULATION DETAILS

Experiment. A HiPCO SWCNT dry powder was purchased from ChemElectronics, Inc. The diameter range of SWCNTs was 0.8–1.2 nm and the quantity of the residue, which was reported as Fe in the sample, was about <35 wt %. According to thermogravimetric analysis (TGA) from the manufacturer, the Fe residue was fully converted into Fe₂O₃ at a temperature higher than 800 °C. All of the specimens in this study were prepared in a graphite filament crucible without further purification (Figure 7).

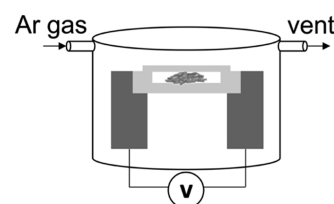


Figure 7. Schematic of the rapid joule heating system.

The temperature of the rapid joule heating system was controlled by alternating current (AC) up to 600 A (Figure 7) and measured by a pyrometer. The SWCNT sample was enclosed inside a graphite filament crucible made of carbon fiber, both sides of which were connected to two electrodes. The current passing through the graphite filament crucible heated the SWCNTs to the desired temperature quickly (in ~10 s) and the maximum temperature reached 3000 °C. The rapid heating system had a very high ramping rate and both the working pressure and the gas environment inside the chamber were controllable. In this study, the ramping rate was set to 10 s and all of the SWCNT samples were heat treated for 10 min in an Ar gas of 770 Torr. After treatment, the sample was dispersed in ethanol with sodium dodecyl sulfate (SDS) for 1 h by ultrasonication. Then, the samples were characterized by Raman spectra with a 532 nm green laser and a transmission electron microscope (TEM).

Modeling and Simulation. The self-developed energy-driven Monte Carlo (EDKMC) method^{13–15} was applied to simulate the coalescence of the SWCNT bundle. In the carbon system, the REBO² potential was used to describe the covalent bonds and van der Waals interactions in and between the carbon layers. As shown in Figure S2, the structure transformation was realized by the random 90° rotations of the C–C bond in the carbon system, which is also called the generalized Stone–Wales (GSW) transformation.¹⁶ The accepted probability of each bond rotation was determined by $\exp(-\Delta E/kT)$, where $\Delta E = E_f - E_i$, E_f and E_i are the energies of the optimized structures after and before the bond rotations, k is the Boltzmann constant, and T is the temperature ($T = 3000$ K). Therefore, we use steps of generalized Stone–Wales (GSW) transformation to reflect the steps of the accepted bond rotations. The detailed running program of EDKMC is shown in Figure S3. In this article, the sequential coalescence of three SWCNTs of (6,6) chiralities (i.e., (6,6) + (6,6) SWCNTs and (6,6) + (12,12) SWCNTs) and the spontaneous coalescence of multiple (6,6) SCWNTs around a large dummy (12,12) SWCNT were simulated. The three initial structures are shown in Figure S1. In these models, the periodic conditions with eight repeated zigzag units (19.68 Å) along the length directions were adopted to mimic the infinite SWCNTs. The atom numbers of (6,6) + (6,6) SWCNTs, (12,12) + (6,6) SCWNTs, and multiple (6,6) SCWNTs around the dummy (12,12) SWCNT were 384, 576, and 1728, respectively. The distance between the two adjacent coalesced SWCNTs was ~1.4 Å.

ASSOCIATED CONTENT

Supporting Information

The Supporting Information is available free of charge at <https://pubs.acs.org/doi/10.1021/acsomega.0c06133>.

Initial structures for simulation (Figure S1); illustration of C–C bond rotation (Figure S2); and running program of the EDKMC method (Figure S3) (PDF)

AUTHOR INFORMATION

Corresponding Author

Feng Ding – School of Materials Science and Engineering, Ulsan National Institute of Science and Technology, Ulsan 44919, Korea; Centre for Multidimensional Carbon Materials, Institute for Basic Science, Ulsan 44919, Korea; orcid.org/0000-0001-9153-9279; Email: f.ding@unist.ac.kr

Authors

Byungcheon Yoo – School of Materials Science and Engineering, Ulsan National Institute of Science and Technology, Ulsan 44919, Korea; Centre for Multidimensional Carbon Materials, Institute for Basic Science, Ulsan 44919, Korea

Ziwei Xu – Centre for Multidimensional Carbon Materials, Institute for Basic Science, Ulsan 44919, Korea; School of Materials Science and Engineering, Jiangsu University, Zhenjiang 212013, China

Complete contact information is available at:

<https://pubs.acs.org/10.1021/acsomega.0c06133>

Notes

The authors declare no competing financial interest.

ACKNOWLEDGMENTS

This work is supported by the Institute for Basic Science (IBS-R019-D1) of South Korea, the Outstanding Research Fund (1.170072.01) of Ulsan National Institute of Science and Technology, the National Natural Science Foundation of China (11774136), and China Scholarship Council program (201908320231).

REFERENCES

- (1) Iijima, S. Helical Microtubules of Graphitic Carbon. *Nature* **1991**, *354*, 56–58.
- (2) Sanchez-Valencia, J. R.; Dienel, T.; Groning, O.; Shorubalko, I.; Mueller, A.; Jansen, M.; Amsharov, K.; Ruffieux, P.; Fasel, R. Controlled Synthesis of Single-Chirality Carbon Nanotubes. *Nature* **2014**, *512*, 61–64.
- (3) Liu, J.; Wang, C.; Tu, X.; Liu, B.; Chen, L.; Zheng, M.; Zhou, C. Chirality-Controlled Synthesis of Single-Wall Carbon Nanotubes Using Vapour-Phase Epitaxy. *Nat Commun* **2012**, *3*, No. 1199.
- (4) Yang, F.; Wang, X.; Zhang, D.; Yang, J.; Luo, D.; Xu, Z.; Wei, J.; Wang, J.-Q.; Xu, Z.; Peng, F.; Li, X.; Li, R.; Li, Y.; Li, M.; Bai, X.; Ding, F.; Li, Y. Chirality-Specific Growth of Single-Walled Carbon Nanotubes on Solid Alloy Catalysts. *Nature* **2014**, *510*, 522–524.
- (5) Shi, Z.; Lian, Y.; Zhou, X.; Gu, Z.; Zhang, Y.; Iijima, S.; Zhou, L.; Yue, K. T.; Zhang, S. Mass-Production of Single-Wall Carbon Nanotubes by Arc Discharge Method. This Work Was Supported by the National Natural Science Foundation of China, No. 29671030. *Carbon* **1999**, *37*, 1449–1453.
- (6) Scott, C. D.; Arepalli, S.; Nikolaev, P.; Smalley, R. E. Growth Mechanisms for Single-Wall Carbon Nanotubes in a Laser-Ablation Process. *Appl. Phys. A: Mater. Sci. Process.* **2001**, *72*, 573–580.
- (7) Nessim, G. D. Properties, Synthesis, and Growth Mechanisms of Carbon Nanotubes with Special Focus on Thermal Chemical Vapor Deposition. *Nanoscale* **2010**, *2*, 1306–1323.
- (8) Bronikowski, M. J.; Willis, P. A.; Colbert, D. T.; Smith, K. A.; Smalley, R. E. Gas-Phase Production of Carbon Single-Walled Nanotubes from Carbon Monoxide via the HiPco Process: A Parametric Study. *J. Vac. Sci. Technol., A* **2001**, *19*, 1800–1805.
- (9) Nikolaev, P.; Thess, A.; Rinzler, A. G.; Colbert, D. T.; Smalley, R. E. Diameter Doubling of Single-Wall Nanotubes. *Chem. Phys. Lett.* **1997**, *266*, 422–426.
- (10) Yudasaka, M.; Kataura, H.; Ichihashi, T.; Qin, L. C.; Kar, S.; Iijima, S. Diameter Enlargement of HiPco Single-Wall Carbon Nanotubes by Heat Treatment. *Nano Lett.* **2001**, *1*, 487–489.
- (11) Méténier, K.; Bonnamy, S.; Béguin, F.; Journet, C.; Bernier, P.; Lamy de La Chapelle, M.; Chauvet, O.; Lefrant, S. Coalescence of Single-Walled Carbon Nanotubes and Formation of Multi-Walled Carbon Nanotubes under High-Temperature Treatments. *Carbon* **2002**, *40*, 1765–1773.
- (12) López, M. J.; Rubio, A.; Alonso, J. A.; Lefrant, S.; Méténier, K.; Bonnamy, S. Patching and Tearing Single-Wall Carbon-Nanotube Ropes into Multiwall Carbon Nanotubes. *Phys. Rev. Lett.* **2002**, *89*, No. 255501.
- (13) Xu, Z.; Li, H.; Fujisawa, K.; Kim, Y. A.; Endo, M.; Ding, F. Multiple Intra-Tube Junctions in the Inner Tube of Peapod-Derived Double Walled Carbon Nanotubes: Theoretical Study and Experimental Evidence. *Nanoscale* **2012**, *4*, 130–136.
- (14) Ding, F.; Yakobson, B. I. Energy-Driven Kinetic Monte Carlo Method and Its Application in Fullerene Coalescence. *J. Phys. Chem. Lett.* **2014**, *5*, 2922–2926.
- (15) Ding, F.; Xu, Z.; Yakobson, B. I.; Young, R. J.; Kinloch, I. A.; Cui, S.; Deng, L.; Puech, P.; Monthieux, M. Formation Mechanism of Peapod-Derived Double-Walled Carbon Nanotubes. *Phys. Rev. B* **2010**, *82*, 41403.
- (16) Stone, A. J.; Wales, D. J. Theoretical Studies of Icosahedral C₆₀ and Some Related Species. *Chem. Phys. Lett.* **1986**, *128*, 501–503.
- (17) Dresselhaus, M. S.; Dresselhaus, G.; Jorio, A.; Souza Filho, A. G.; Saito, R. Raman Spectroscopy on Isolated Single Wall Carbon Nanotubes. *Carbon* **2002**, *40*, 2043–2061.
- (18) Zhang, G.; Qi, P.; Wang, X.; Lu, Y.; Li, X.; Tu, R.; Bangsaruntip, S.; Mann, D.; Zhang, L.; Dai, H. Selective Etching of Metallic Carbon Nanotubes by Gas-Phase Reaction. *Science* **2006**, *314*, 974–977.
- (19) Yudasaka, M.; Ichihashi, T.; Kasuya, D.; Kataura, H.; Iijima, S. Structure Changes of Single-Wall Carbon Nanotubes and Single-Wall Carbon Nanohorns Caused by Heat Treatment. *Carbon* **2003**, *41*, 1273–1280.